

# Experimental evaluation of novel precast concrete beam-to-column moment connections for enhanced collapse resistance

Malcolm L. Ammons, Jonathan M. Weigand, Majd Hijazi, and Travis E. Thonstad

**D**isproportionate collapse is a phenomenon characterized by local damage or failure of a relatively small part of a structure that leads to collapse of the entire structure or a large part of it.<sup>1</sup> A notable instance of disproportionate collapse occurred on May 16, 1968, at the Ronan Point apartment tower in London, England, when a small gas explosion on the 18th floor precipitated collapse of 22 stories of corner apartments at the southeast corner of the building. That incident led to the first changes to U.K. building regulations that specifically aimed to prevent disproportionate collapse.<sup>2</sup> The September 11, 2001, collapse of the World Trade Center Towers 1 and 2 in New York, N. Y., following impacts from two commercial airliners, provided additional motivation to the engineering community and regulatory bodies to develop design methods and robust structural systems capable of resisting disproportionate collapse.<sup>3</sup> The idea behind robust structural systems is that unanticipated loads that are not explicitly considered in design (for example, loads from an explosion, vehicle impact, or material degradation) should not lead to the collapse of all or a large part of a building.

The National Institute of Standards and Technology (NIST) has experimentally and computationally researched disproportionate collapse for years, examining the collapse resistance of various moment frame systems composed of cast-in-place reinforced concrete,<sup>4</sup> steel,<sup>5</sup> and precast concrete.<sup>6</sup> The current study builds on some of NIST's more recent work, specifically, the connections presented in this paper were developed in part to address shortcom-

- The study presents experimental data that characterize the behavior of novel precast concrete beam-to-column moment connections subjected to loading that could initiate disproportionate collapse.
- The test assemblies were produced at a five-eighth scale based on a 10-story prototype building and consisted of two spandrel beams connected to a central column. The two precast concrete assemblies used either anchor bolts or threaded rods and did not require field welding.

ings observed from experimental testing of full-scale precast concrete assemblies of moment-resisting spandrel beam-to-column connections by Main et al.<sup>6</sup> In that recent study, the investigators tested two types of assemblies under a simulated column-removal scenario. One of the assemblies had detailing that met special moment frame requirements, and the other had detailing that met ordinary moment frame requirements. Both assemblies had precast concrete beam-to-column moment connections made by steel link plates, which were fillet welded to steel angles embedded in the beams and then fillet welded to plates embedded in the columns. Standard connection details for precast concrete seismic applications<sup>7</sup> were used in both assemblies, therefore the assemblies' ability to resist disproportionate collapse was unknown. An energy-based analysis of the test results found that both assemblies had a small margin of safety against collapse under sudden column loss considering applicable gravity loads. Main and coauthors<sup>6</sup> identified two modifications that would likely improve the performance of the connections:

- reducing eccentricities of the tensile force transfer path
- limiting the use of field welding to make connections between critical components because weld quality is difficult to control in the field

Motivated by the small margin of safety against collapse of the tested precast concrete assemblies, NIST identified several alternative connection concepts in coordination with an industry review committee of PCI members. These alternative connection concepts were intended to address the potential vulnerabilities in the welded link plates identified during testing, thereby improving the robustness of the connections.

One of the alternative connection concepts used high-strength threaded rods that pass from one beam through the column and into the adjacent beam and are connected using embedded couplers within the column. The threaded rods replace the welded link plates and, when placed at the center of the spandrel beams' cross sections, eliminate tension-load-path eccentricities. Investigators have assessed the performance of this type of connection concept under different loading scenarios. French et al.<sup>8,9</sup> investigated the seismic behavior of precast concrete beam-to-column moment connections subjected to cyclic loads that used grouted high-strength rods and threaded couplers. The connection assemblies exhibited ductile behavior but had concrete crushing in the breakout regions of the spandrel beams where the rods were anchored.

Quiel et al.<sup>10</sup> investigated a similar concept but tested two connection assemblies under a notional column-removal scenario, each with a different diameter of high-strength rod. In their work, the high-strength rods passed continuously from one beam through the column and into the adjacent beam, with the rods being ungrouted and anchored by nuts that bore against anchorage blocks on the interior face of each beam. The anchorage blocks exhibited substantial distress during testing, as indicated by spalling and crushing of the concrete, but the

study's numerical analysis of the prototype building frame from which the assemblies were derived indicated that both connections were able to arrest collapse in a scenario where a single column was lost. The connection concepts detailed in this paper are similar to those previously described and have novel design and detailing features aimed at achieving robust performance against disproportionate collapse.

The goal of the study reported herein was to generate experimental data that characterize the behavior of novel precast concrete beam-to-column moment connections subjected to loading that could initiate disproportionate collapse (that is, a column-removal scenario). This paper presents experimental results for two moment connections that used either anchor bolts or threaded rods. Data generated from this study can be used to validate nonlinear computational models of entire precast concrete moment-framed buildings to ascertain which connection will most effectively arrest disproportionate collapse and minimize building damage under notional removal of a column.

## Prototype building design

The connection assemblies described in this paper were based on a 10-story prototype precast concrete office building designed by S. K. Ghosh and Associates in 2009.<sup>11</sup> The building was designed assuming a location in Seattle, Wash., with site Class D. The building was classified as seismic design category D and occupancy category II. The lateral-load-resisting system consisted of perimeter special moment frames in each orthogonal in-plan direction. The floor system consisted of double tees spanning the north-south directions and resting on inverted tee beams spanning the east-west directions. The design specified a normalweight cast-in-place concrete topping slab with a thickness ranging from 2.50 to 3.50 in. (64 to 89 mm) to account for camber in the double tees. In addition to self-weight, a superimposed dead load of 10 lb/ft<sup>2</sup> (0.48 kN/m<sup>2</sup>) and a live load of 100 lb/ft<sup>2</sup> (4.79 kN/m<sup>2</sup>) were considered for a typical floor. The live load was reduced in accordance with the American Society of Civil Engineers' Minimum Design Loads for Buildings and Other Structures (ASCE 7-05).<sup>12</sup> The connection assemblies that were tested are representative of the third-story moment frame assembly shown in **Fig. 1**, which shows plan and elevation views of the prototype building from which the experimental assemblies were derived. The elevation view of the prototype building (**Fig. 1**) highlights the extracted moment frame assembly that was considered for the experimental tests described in this paper.

## Connection concepts

**Figure 2** shows test assemblies featuring the two connection concepts investigated in this study—bolted and threaded rod—along with their steel reinforcement details and the locations of strain gauges applied to the reinforcing bars before the concrete was cast. Due to laboratory constraints, the dimensions of the test assemblies were scaled to five-eighths

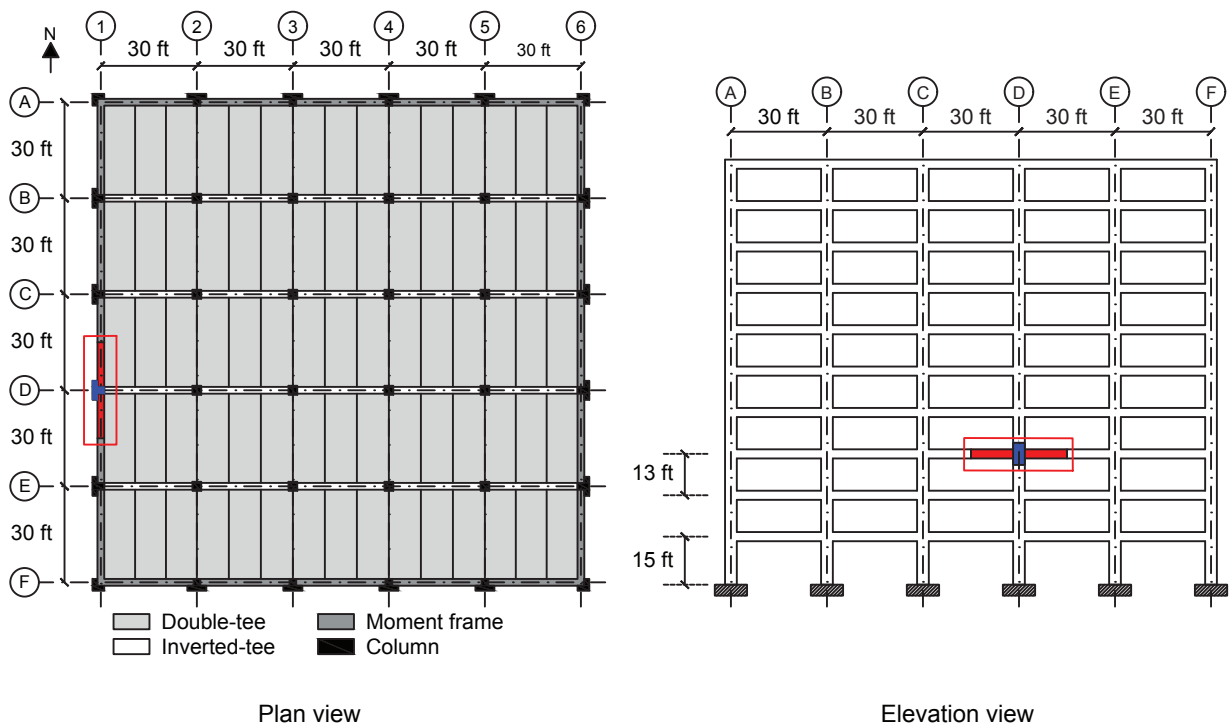


**Figure 1.** The 10-story prototype building for the tested moment frame assemblies. Note: 1 ft = 0.305 m.

of those of the prototype building. The spandrel beams for the tested assemblies extended to half the scaled bay width on either side of the column, which corresponded to the location of assumed inflection points under a notional column-loss scenario. The height of the portion of the column between spandrel beams was determined by the clearance available underneath the assembly, which needed to be large enough to permit significant rotation of the beam connections. Using a column height in the specimens that was less than five-eighths of the prototype building third-story height was deemed acceptable, since the column's primary function in the tests was to transfer force into the connection, and a longer column would not have an appreciable effect on the connection behavior.

The factored moment demand at the beam-to-column connection for the prototype scale was 959 kip-ft (1301 kN-m). This value was calculated using the extraordinary events load case ( $1.2D + 0.5L + A_k$ , where  $D$  is dead load,  $L$  is live load, and  $A_k$  is the load or load effect resulting from the extraordinary event) from ASCE 7-16,<sup>13</sup> and a 1.2 dynamic amplification factor calculated using the U.S. Department of Defense's *Unified Facilities Criteria: Design of Buildings to Resist Progressive Collapse* (UFC 4-023-03).<sup>14</sup> For geometric similitude with length scale  $S_L$  of  $\frac{5}{8}$  and stress scale  $S_\sigma$  of 1, the moment demand scale  $S_M = S_L \times S_L \times S_L \times S_\sigma = 0.244$ , which results in a moment demand for the scaled connection assembly of 234 kip-ft (317 kN-m).

Testing the connection assemblies at less than full scale was expected to minimally influence the test results because the connection assemblies and associated design forces and moments were properly scaled from the prototype structure using geometric similitude and dimensional analysis. Testing at full scale would have likely facilitated fabrication of the beams and columns at the precast concrete plant and assembly of the connections in the laboratory. Clearances would increase, and precast concrete plants are accustomed to fabricating components at full scale. Furthermore, the increased sizes of the beams, columns, and connection components would presumably create more space (for example, larger hand holes) to align and make the connections and to ensure that the steel reinforcement and connection components do not become congested.

Both connection concepts relied on threaded rods to transfer moments between the beams and column. Beam longitudinal reinforcement was welded to embedded steel boxes near the ends of the beams. The threaded rods passed through voids in the beams and were anchored against the embedded steel boxes and coupled within the column. The main difference between the two connection concepts was the length of threaded rods and the attendant grade of steel necessary to achieve similar connection rotations before fracture. The steel deformed bar reinforcement for both connections was ASTM A706 Grade 60 (414 MPa).<sup>15</sup> The specimens were assembled by sliding the threaded rods through voids in the beam ends

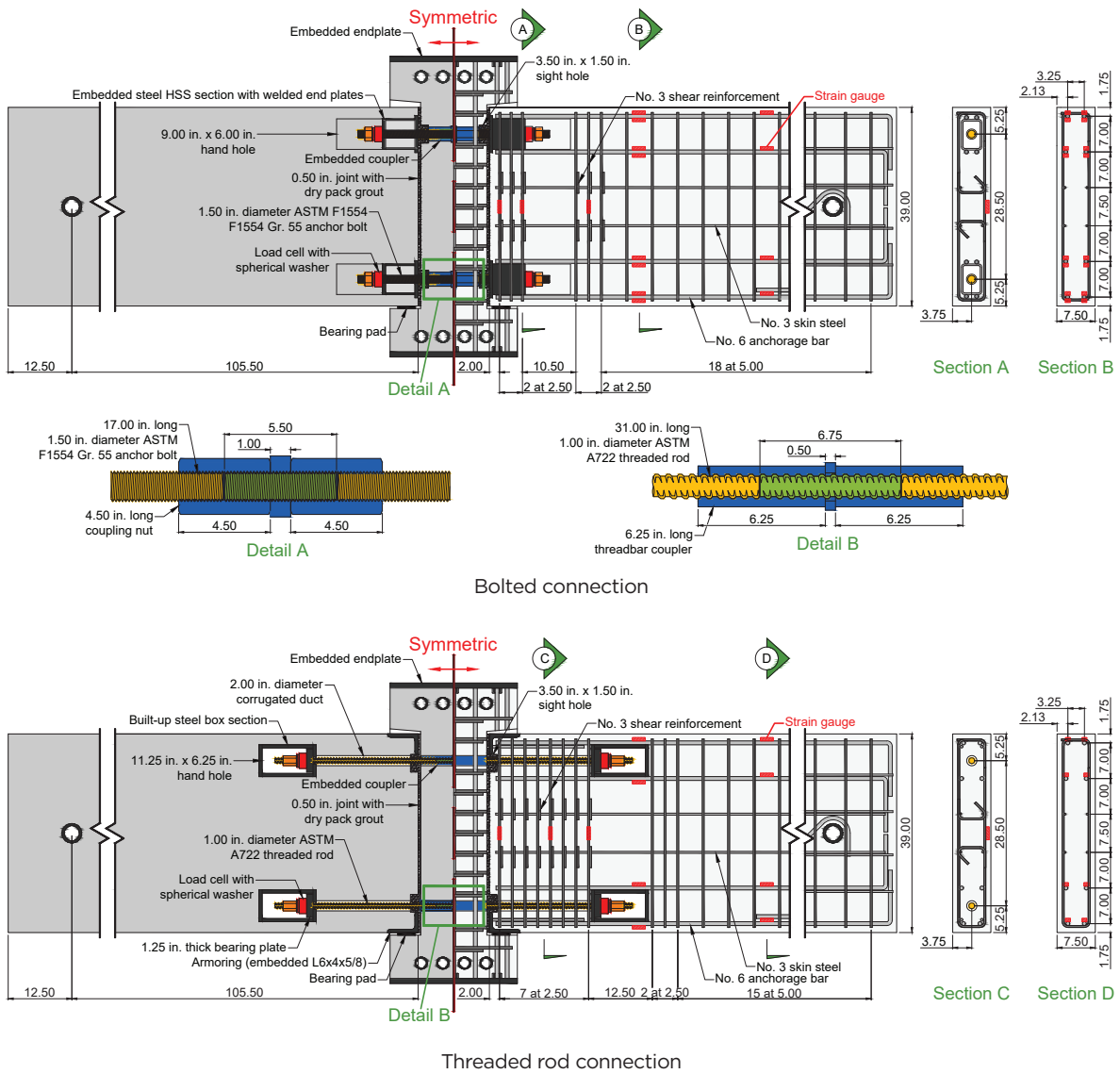


**Figure 2.** Schematic of the bolted and threaded rod connection concepts illustrating their skin steel reinforcement details and locations of embedded strain gauges. Note: All dimensions shown in inches. No. 6 = 19M; 1 in. = 25.4 mm.

created by either hollow structural sections for the bolted connection or 2.00 in. (51 mm) diameter corrugated ducts for the threaded rod connection, placing the beam ends on 0.50 in. (13 mm) thick bearing pads that were in the column pockets, and then threading the bars into the couplers embedded in the column.

The bolted connection was based on a connection concept shown in the *PCI Design Handbook: Precast and Prestressed Concrete*.<sup>16</sup> The bolted connection used 1.50 in. (38 mm) diameter, fully threaded Grade 55 (379 MPa) anchor bolts produced in accordance with ASTM F1554-20.<sup>17</sup> The anchor bolts had a specified tensile strength between 75 and 95 ksi (517 and 655 MPa). The length of bar used for this connection was 17 in. (432 mm), as opposed to 31 in. (787 mm) for the threaded rod connection, there-

fore a lower-strength steel was necessary to achieve the target connection rotational capacity of 2.30 degrees. The target connection rotational capacity was selected based on acceptance criteria for experimental evaluation of innovative seismic moment frames presented in the American Concrete Institute's *Acceptance Criteria for Moment Frames Based on Structural Testing and Commentary* (ACI 374.1-05).<sup>18</sup> The bolted connection was made by passing the anchor bolt through the rectangular steel hollow structural sections embedded within the beams, which then terminated in coupling nuts embedded in the column. Similar to the threaded rod connection, the bolted connection had beam longitudinal reinforcing welded to the tops and bottoms of the hollow structural sections to allow forces in the anchor bolts to be transferred to the beams. The two coupling nuts embedded near the top and bottom of the column were mated with a

5.50 in. (140 mm) long anchor bolt and tightened against a 1.00 in. (25 mm) thick plate washer made from ASTM A36 steel.<sup>19</sup> The connection was completed by threading a nut on the end of the anchor bolts and dry-packing the interface between the beams and column with cementitious nonshrink grout. Tensile force in the anchor bolts was measured by through-hole (donut) compression load cells that were sandwiched between the nuts and a 0.63 in. (16 mm) thick steel plate welded to the end of the hollow structural sections (Fig. 2). Spherical washers were employed between the through-hole load cells and nuts to compensate for any lack of perpendicularity in the bearing surfaces.

For the threaded rod connection, a moment-resisting connection was established by mating high-strength thread bar with cylindrical couplers that were embedded in the column. The two cylindrical couplers embedded near the top and bottom of the column were mated with a 6.75 in. (171 mm) length of thread bar and tightened against a 0.50 in. (13 mm) thick plate washer made from ASTM A36 steel.<sup>19</sup> The 1.00 in. (25 mm) diameter (nominal) Type II high-strength thread bar, which was produced in accordance with ASTM A722/A722M-18,<sup>20</sup> had a minimum specified yield strength of 120 ksi (827 MPa) and a minimum specified tensile strength of 150 ksi (1034 MPa). The cylindrical couplers were advertised as being capable of developing the ultimate strength of the thread bar. The connection was established by first sliding the 1.00 in. diameter (nominal) thread bars through 2.00 in. (51 mm) diameter corrugated duct embedded within the beams, placing the beam ends on 0.50 in. thick bearing pads that were in the column pockets, and then threading the bars into the couplers embedded in the column. The thread bars were tightened by hand with the occasional use of a strap wrench. The connection was completed by anchoring a hex nut on the end of each thread bar and then dry packing the beam-column interface with nonshrink cementitious grout. Axial forces in the thread bars were transferred into the beams by bearing of the embedded built-up steel box sections within the beams and steel reinforcing bars welded to the top and bottom of the built-up sections. Tensile force in the thread bars was measured by through-hole compression load cells that were sandwiched between the hex nuts and 1.25 in. (32 mm) thick steel bearing plates (Fig. 2). Spherical washers were used between the load cells and nuts, as was done for the bolted connection.

To limit the eccentricity of force transfer between connection components, both the bolted and threaded rod connections used components that were centered on the beam thickness. During the full-scale experimental tests conducted previously by NIST,<sup>6</sup> the eccentricity of tensile force transfer introduced localized out-of-plane bending and played a critical role in the premature fracture of the anchorage bars. Both the bolted and threaded rod connections also eliminated the need to weld critical components on-site.

Construction tolerances do not properly scale, and thus care should be taken in interpreting observations about constructibility in the laboratory; however, each connection was found

to have advantages and disadvantages during assembly of the specimens. The longer length, smaller diameter, and coarser threads (two threads per 1.00 in. [25 mm] of length) of the thread bars used for the threaded rod connection permitted greater flexibility and maneuverability in establishing the connection. The finer threads of the anchor bolts used for the bolted connection (six threads per 1.00 in. of length) were susceptible to damage during fit up, making them difficult to thread smoothly and fully into the coupling nuts. A tap and die were necessary to clean the threads of the nuts and anchor bolts, respectively, to ensure that the pair could be mated during construction. A pipe wrench was needed to thread the anchor bolts into the coupling nuts because the coupling nuts might have slightly shifted during casting, resulting in the bottom anchor bolts being inclined from horizontal and skewed out of the plane of the connection.

## Experimental program

### Test setup

**Figure 3** shows the test setup for the static pushdown tests. The assemblies were tested using a single-span portal frame with a servohydraulic actuator mounted to the underside of its cross beam. The precast concrete column was attached to the actuator loading plate using four high-strength threaded rods that threaded into nuts embedded at the top of the column. The actuator displaced the unsupported column downward in 0.25 in. (6 mm) increments at a rate of 0.20 in./min (5 mm/min). Loading was paused after each increment to allow for photographs to be taken and cracks to be highlighted with permanent marker. The end of the spandrel beams away from the connection were connected to steel cradles via a 3.00 in. (76 mm) diameter steel pin. The cradles rested on a low-friction sliding surface, which allowed them to slide freely in the plane of the connection. The force from the actuator was transmitted into the strong floor through a steel foundation frame. A lateral bracing system that attached to the foundation frame via high-strength bolts ensured that the column displaced vertically, while simultaneously permitting in-plane rotation of the connection. This experimental configuration tested the connections under flexure with minimization of axial and torsional forces. Although the spandrel beams would be subjected to flexural, axial, and torsional forces during an actual column-removal scenario, NIST's previous full-scale tests of precast concrete moment frame connection assemblies showed that the flexural response assumed a dominant role in arresting collapse; therefore, the flexural response of the connection assemblies was considered most important to investigate.

### Instrumentation

**Figure 4** presents a schematic of the instrumentation layout. The force applied to the assembly by the actuator was measured using four through-hole compression load cells that were sandwiched between the actuator loading plate

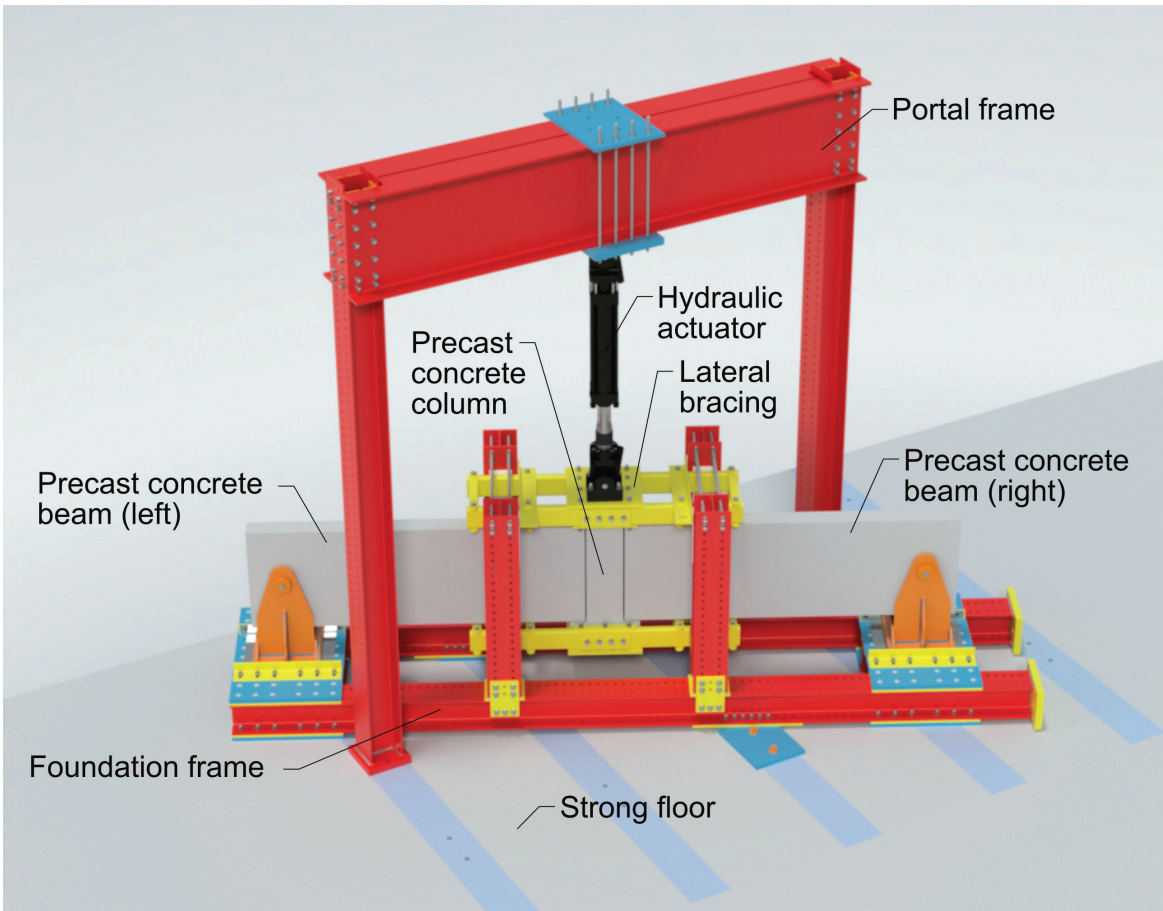


**Figure 3.** Connection test setup.

and the plate embedded at the top of the column. The load cells (LC01 through LC04) were preloaded to approximately 15 kip (66.7 kN) each to ensure that they remained in compression for the duration of the test. Vertical displacement of the assembly was measured by 10 string potentiometers (D01 through D10) that were mounted to aluminum beams located above the spandrel beams and oriented parallel to the span of the precast concrete beams. Axial elongation and contraction of the spandrel beams near the connection were measured using four linear variable inductance transducers (T01 through T08) mounted to each beam, two on the top side of the beam and two on the bottom side. Five inclinometers (R01 through R05) were mounted to the front surface of the beams and column to measure in-plane rotation. Two linear variable displacement transducers (L11 and L12), one at the bottom of each steel cradle, were used to measure cradle displacement. Uniaxial strain gauges were adhered to the surface of the reinforcing steel in the spandrel beams to measure strain (Fig. 2). These strain gauges were applied before the concrete was cast at the precaster's plant. Strain gauges also were adhered to the thread bars in the laboratory to capture surface strains. These strain gauges were attached to the top and bottom sides of the thread bars, 4.50 in. (114 mm) from their ends,

which were embedded in the column. Strain gauges were not applied to the anchor bolts because there was no appropriate surface on which to adhere them. **Table 1** shows the estimated total expanded uncertainty of the measured forces, rotations, displacements, and strains, which were calculated using a coverage factor  $k$  of 2. The uncertainties in Table 1 apply to all measurements presented in the experimental results section of this paper.

## Material properties

All beams and columns were cast consecutively on the same day from the same concrete batch and mixture proportions. A concrete compressive strength of 6000 psi (41.4 MPa) with an expected compressive strength of 9000 psi (62.1 MPa) was specified for the design of the precast concrete components. The 28-day compressive strength of the concrete, tested in accordance with ASTM C39-21<sup>21</sup> and based on six breaks of 4 × 8 in. (102 × 203 mm) cylinders, was 8050 ± 200 psi (55 ± 1.4 MPa), where 8050 psi is the mean value  $\mu$  of the six break strengths, and 200 psi is the expanded uncertainty  $U$ . The expanded uncertainty is calculated using Eq. (1).

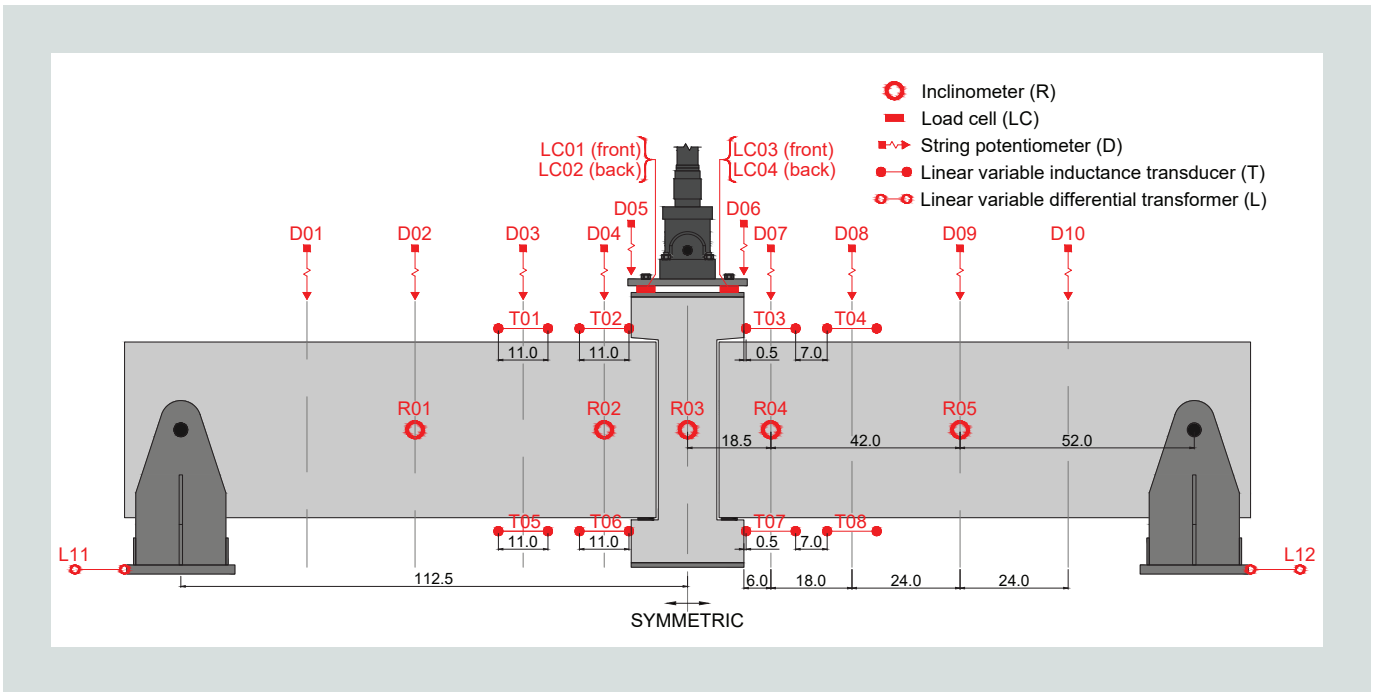


**Figure 4.** A schematic of the instrumentation layout. Note: All dimensions shown in inches. 1 in. = 25.4 mm.

**Table 1.** Measurement uncertainty

Measurement	Measurement device	Measuring range	Estimated expanded uncertainty
Distance, in.	Tape measure	300	0.06
Strain, %	Resistance-based strain gauge	-10	1
Vertical displacement, in.	String potentiometer	20	0.08
Horizontal displacement, in.	Linear variable displacement transducer	4	0.02
Horizontal displacement, in.	Linear variable inductance transducer	2	0.01
Rotation, degrees	Inclinometer	±10	0.05
Compressive force, kip	Load cell	190	1.5
Moment, kip-ft	Derived quantity	1670	14.1

Note: 1 in. = 25.4 mm; 1 kip = 4.448 kN; 1 kip-ft = 1.356 kN-m.

$$U = \frac{ku_c}{\sqrt{n}} \tag{1}$$

where

- $k$  = coverage factor calculated using the two-tailed student's  $t$  distribution to define an interval in which the true mean lies with a level of confidence of 95%
- $u_c$  = sample standard deviation
- $n$  = number of independent measurements

The material strength values in this section are presented in

the form  $\mu \pm U$ . The concrete compressive strength on test day was  $9380 \pm 190$  psi ( $65 \pm 1.3$  MPa) for the threaded rod connection assembly and  $9140 \pm 350$  psi ( $63 \pm 2.4$  MPa) for the bolted connection assembly.

Two batches of dry-pack cementitious grout were used to pack the beam-to-column interface for each connection assembly, one batch for the interface to the left of the column and one batch for the interface to the right of the column. Grout cubes were made and tested in accordance with ASTM C109-21<sup>22</sup> and ASTM C1107/C1107M-20.<sup>23</sup> For the threaded rod assembly, the average compressive strength of the grout based on two grout cubes each for the interface to the left and right of the column was  $10,430 \pm 1290$  psi ( $71.9 \pm 8.9$  MPa)

for the interface to the left and  $9780 \pm 610$  psi ( $67.4 \pm 4.2$  MPa) for the interface to the right. For the bolted connection assembly, the average compressive strength of the grout based on two grout cubes each for the interface to the left and right of the column was  $9540 \pm 1490$  psi ( $65.8 \pm 10.3$  MPa) for the interface to the left and  $10,190 \pm 1980$  psi ( $70.3 \pm 13.7$  MPa) for the interface to the right.

To characterize the behavior of the thread bars and anchor bolts, monotonic tension tests were conducted using a servo-hydraulic load frame. Two 31 in. (787 mm) long thread bars and two 17 in. (432 mm) long anchor bolts were tested. Their lengths corresponded to the lengths of the bars used in the experimental tests. The bars were tested in force control at a rate of 25.0 kip/min (111 kN/min) up to half the minimum specified yield strength. Loading was then continued in displacement control at a rate of 0.25 in./min (6 mm/min) until bar rupture. An extensometer with an 8 in. (203 mm) gauge length was attached near the midlength of each bar to measure strain. The average yield strength was  $143 \pm 19.7$  ksi ( $986 \pm 136$  MPa) for the thread bars and  $71.3 \pm 1.3$  ksi ( $492 \pm 8.96$  MPa) for the anchor bolts. Yield strength was calculated using the 0.2% offset method. The average tensile strength was  $160 \pm 2.4$  ksi ( $1103 \pm 16.5$  MPa) for the thread bars and  $89.8 \pm 1.9$  ksi ( $619 \pm 13.1$  MPa) for the anchor bolts. For all tests, stress was calculated by dividing the force measured by the in-line load cell of the load frame by the cross-sectional area specified in the corresponding ASTM standard. The cross-sectional area was taken as  $0.85$  in<sup>2</sup> ( $548$  mm<sup>2</sup>) for the thread bars (in accordance with ASTM A722/A722M-18<sup>20</sup>)

and as  $1.405$  in<sup>2</sup> ( $674$  mm<sup>2</sup>) for the anchor bolts (in accordance with ASTM F1554-20<sup>17</sup>).

## Experimental results

Figure 5 shows a plot of the applied connection moment versus beam chord rotation up to connection failure. The applied connection moment was derived using the force applied to the column in conjunction with shear and moment mechanics, which assumed plastic hinge formation at the beam ends, 105.5 in. (2680 mm) from the center of the pin connections. The moment due to the weight of the assembly was not considered in the applied connection moment calculation because it accounts for less than 5% of the maximum applied connection moment for each assembly. Vertical displacement of the center column was based on the average displacement measurements from two string potentiometers attached to the top of either side of the column. Beam chord rotation  $\theta$  was then calculated using the following equation:

$$\theta = \tan^{-1} \left( \frac{\delta}{L_1} \right)$$

where

$\delta$  = average of two vertical displacement measurements from D05 and D06

$L_1$  = distance from centerline of column to centerline of pin (112.5 in. [2858 mm])

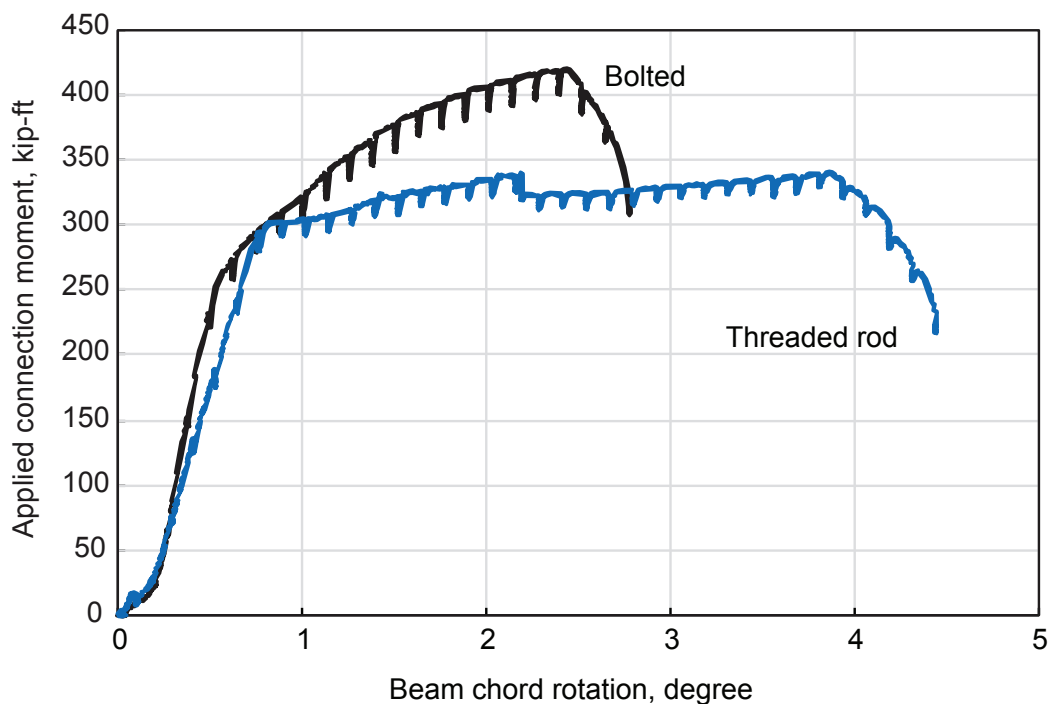


Figure 5. Applied connection moment versus beam chord rotation for both connection assembly tests. Note: 1 kip-ft = 1.356 kN-m.

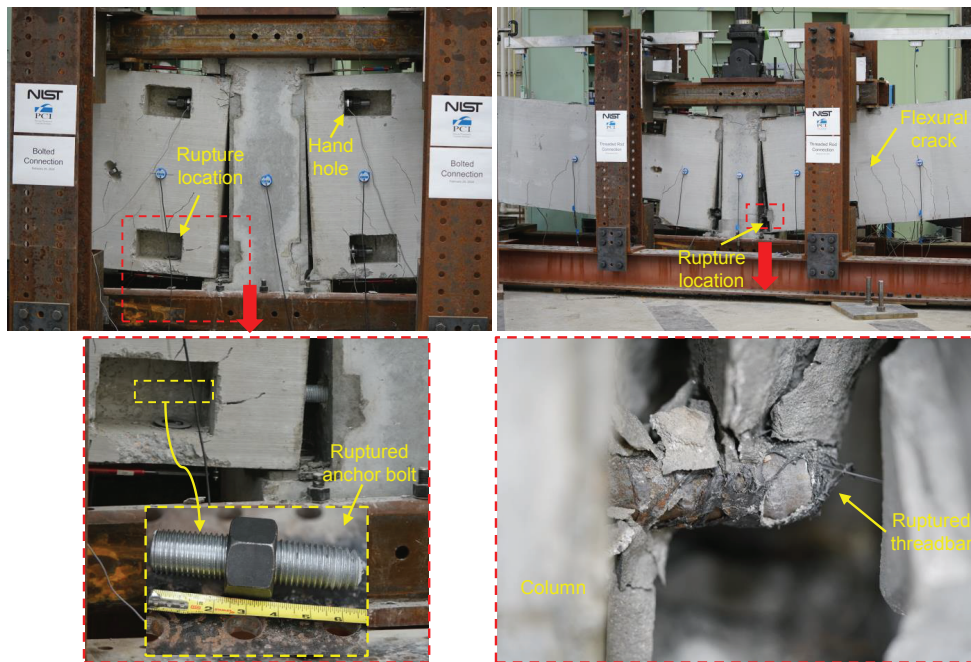
The initial moment-rotation responses for both connection assemblies were linear. Those responses were followed by increases in strength until the connection assemblies' ultimate moment capacities were achieved, and then decreases in strength until fracture occurred in one of the bars that were in tension at the bottoms of the connections. The bolted connection assembly remained linear up to approximately 0.53 degrees of chord rotation and a moment of approximately 250 kip-ft (339 kN-m), whereas the threaded rod connection assembly remained linear up to approximately 0.73 degrees of chord rotation and a moment of 302 kip-ft (409 kN-m). Both connection assemblies initially had a similar stiffness up to 0.27 degrees of chord rotation, after which their stiffnesses began to deviate. The stiffness of the bolted connection assembly was approximately 50% greater than that of the threaded rod connection assembly. This difference can likely be partially attributed to the greater flexural stiffness of the larger diameter anchor bolts compared with that of the thread bars. The bolted connection assembly achieved an ultimate moment of 419 kip-ft (568 kN-m) at a chord rotation of 2.43 degrees, which is 6% greater than the 2.29 degree chord rotation that the connection was designed to achieve. In contrast, the threaded rod connection assembly achieved an ultimate moment of 340 kip-ft (461 kN-m) at a chord rotation of 3.87 degrees. Using the chord rotation at the ultimate moment capacity to quantify the rotational capacity of the assembly, the rotational capacity of the threaded rod connection assembly was nearly 60% higher than that of the bolted connection assembly. However, this increase in rotational capacity came at a sacrifice of strength and stiffness: the stiffness of the bolted connection assembly was approximately 50% greater than that of the threaded rod connection assembly and the bolted connection assembly had approximately 23% greater moment capacity. Note that these comparisons of rotational capacity, stiffness, and strength are only valid for the measurements made for the two tested connection assemblies. No replicate connection assemblies were fabricated or tested to understand the potential for specimen-to-specimen variations in rotational capacity, stiffness, or strength.

For the bolted connection assembly, flexural cracking in the spandrel beams was initiated during the vertical column displacement increment from 0.75 to 1.00 in. (19 to 25 mm), which corresponded to a change in chord rotation from 0.27 to 0.38 degrees. This initial cracking consisted of one flexural crack near midspan of the right spandrel beam on its front face, with the crack initiating at the bottom of the beam and extending about halfway up its depth. Flexural cracking was not immediately observed in the left beam, as the beam was resting on the bottom anchor bolt and thus deformation was first concentrated in the anchor bolt as the column displaced downward. During the vertical column displacement increment from 1.25 to 1.50 in. (32 to 38 mm), which corresponded to a change in chord rotation from 0.50 to 0.62 degrees, the bolted assembly response transitioned from linear to nonlinear and numerous flexural cracks occurred near midspan of both spandrel beams on their front (which would be the interior building

face) and back faces. During the vertical column displacement increment from 2.25 to 2.50 in. (57 to 64 mm), which corresponded to a change in chord rotation from 1.00 to 1.13 degrees, the top corners of both beams began to bear firmly on the grout, generating compressive forces in the column that led to cracking and spalling on its left and right sides. The subsequent vertical column displacement increment from 2.50 to 2.75 in. (57 to 70 mm), which corresponded to a change in chord rotation from 1.13 to 1.26 degrees, was accompanied by audible sounds of crushing and spalling of the column at its top end near the top corners of the beams. As loading continued, the gap between the bottom corner of the left beam and the grout grew at a rate that outpaced the growth of the gap on the right side of the assembly, eventually leading to tensile rupture of the bottom-left anchor bolt near the inner face of the hand hole at a vertical column displacement of 5.46 in. (139 mm), which corresponded to 2.78 degrees of chord rotation. Photographs of the failure mode of the bolted connection are shown in the left part of **Fig. 6**.

Hairline flexural cracks were initiated at the bottom front and back faces of both spandrel beams of the threaded rod assembly during the vertical column displacement increment from 1.00 to 1.25 in. (25 to 32 mm), which corresponded to a change in chord rotation from 0.41 to 0.52 degrees. The cracks began extending upward toward the tops of the beams with increased loading. During the vertical column displacement increment from 1.50 to 1.75 in. (38 to 44 mm), which corresponded to a change in chord rotation from 0.64 to 0.76 degrees, the assembly response transitioned from linear to nonlinear. During the vertical column displacement increment from 2.25 to 2.50 in. (57 to 64 mm), which corresponded to a change in chord rotation from 1.02 to 1.14 degrees, the right end of the top of the left beam began to bind, leading to minor spalling in the column at the top left pocket. In the next increment, spalling at the top of the right column pocket occurred. Gaps at the bottom of the beams between the beam ends and the grout interface widened symmetrically until the vertical column displacement increment from 4.50 to 4.75 in. (114 to 121 mm), which corresponded to a change in chord rotation from 2.16 to 2.29 degrees. During that increment, the gap at the bottom right was approximately 0.13 in. (3 mm) larger than the gap at the bottom left and the bottom-right gap continued to increase at a higher rate. A reduction in moment occurred at a vertical column displacement of 4.30 in. (109 mm), which corresponded to a chord rotation of 2.19 degrees. This reduction in moment was associated with a loud noise emitted from one of the thread bars, which was potentially caused by slippage of the thread bar. With continued loading, deformation continued to concentrate at the bottom-right connection until tensile rupture of the bottom-right thread bar occurred near the beam end at a vertical column displacement of 8.74 in. (222 mm), which corresponded to a chord rotation of 4.44 degrees. Photographs of the failure mode of the threaded rod connection are shown in the right part of **Fig. 6**.

**Figure 7** shows vertical displacement profiles from both connection assemblies based on measurements from the 10



Bottom left anchor bolt near the inner face of the hand hole for the bolted connection assembly

Bottom right thread bar near the beam end for the threaded rod connection assembly

**Figure 6.** Tensile rupture failure modes.

symmetrically placed string potentiometers shown in Fig. 4. The column centerline corresponds to a spanwise distance of 0 in. (0 mm), with positive distances indicating measurements taken to the right of the centerline and negative distances indicating measurements taken to the left of the centerline. The left part of Fig. 7 shows five different displacement profiles corresponding to different points in the loading of the bolted connection assembly. Beginning at the first displacement profile and moving sequentially to the last profile from smallest to largest vertical displacements, the profiles correspond to approximately midway through the linear region of assembly response ( $\theta = 0.34$  degrees), the transition point from linear to nonlinear response ( $\theta = 0.53$  degrees), the end of the increment in which column spalling initiated ( $\theta = 1.13$  degrees), ultimate moment ( $\theta = 2.43$  degrees), and the instant just before fracture of the bottom-left anchor bolt ( $\theta = 2.78$  degrees). Asymmetry of the displacement profile is apparent, with larger displacements on the left side of the column than on the right side. The asymmetry grew with increasing vertical column displacement, eventually leading to fracture of the bottom-left anchor bolt.

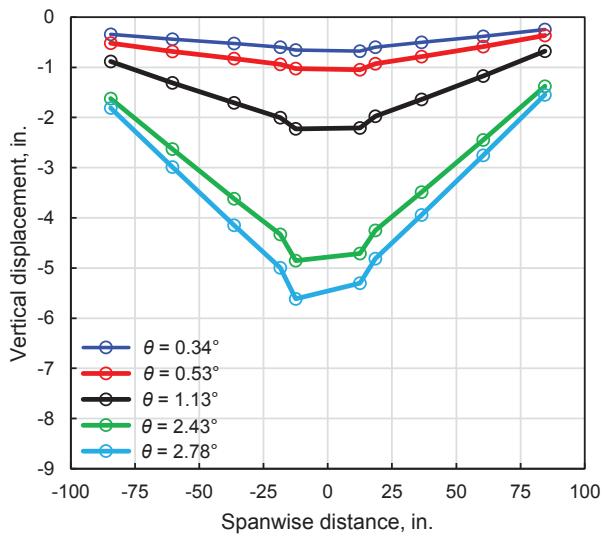
The right part of Fig. 7 shows five different displacement profiles corresponding to different points in the loading of the threaded rod connection assembly. In order of increasing displacement, the profiles correspond to approximately midway through the linear response region ( $\theta = 0.36$  degrees), the transition from linear to nonlinear response ( $\theta = 0.73$  degrees), the point at which there was a sudden drop in force or moment ( $\theta$

$= 2.19$  degrees), the ultimate moment ( $\theta = 3.87$  degrees), and the instant just before fracture of the bottom-right thread bar ( $\theta = 4.44$  degrees). In the linear response region, the displacement profile was fairly symmetric; however, with increasing vertical column displacement, the column began to rotate clockwise within the plane of the connection, leading to a concentration of axial deformation at the bottom-right connection that eventually led to fracture of the bottom-right thread bar.

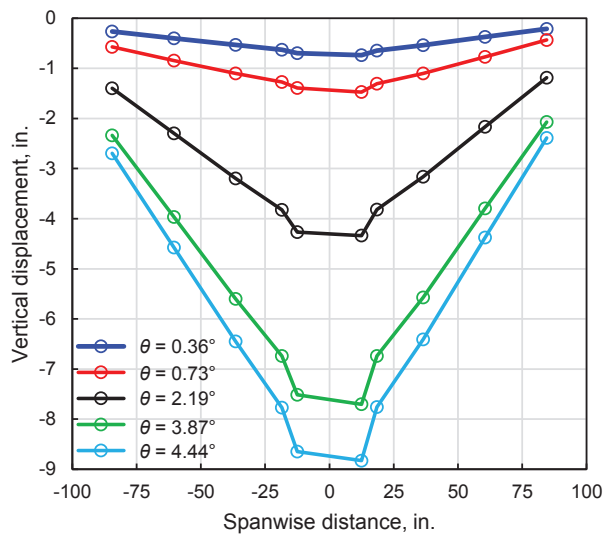
## Rotation

**Figure 8** shows measured in-plane beam rotations for both connection assemblies plotted as a function of vertical displacement of the column. Clockwise rotations are shown as positive, and counterclockwise rotations are shown as negative. The beam rotations were measured with inclinometers, which were positioned as shown in Fig 4. Figure 8 also shows the plotting of beam chord rotations calculated using Eq. (1). The beam chord rotation curve appears twice on each plot, once for positive values of rotation and once for negative values, to provide a basis to compare with inclinometer measurements to determine the occurrence of rigid body rotation.

The curves indicating rotation measurements from inclinometers on the left beam (R01 and R02) and right beam (R04 and R05) of the bolted connection assembly are essentially the same as the curves for the beam chord rotation. This finding indicates that the beams were undergoing rigid body rotations

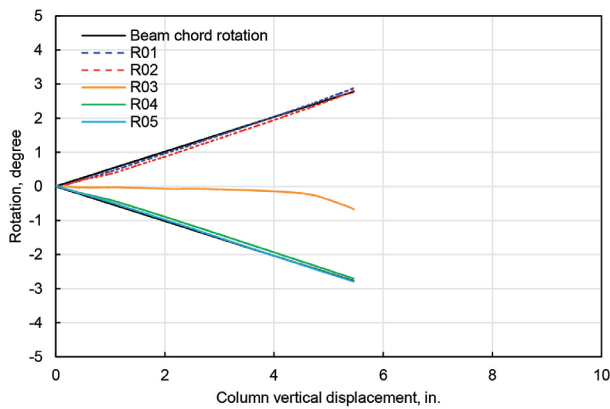


Bolted connection assembly

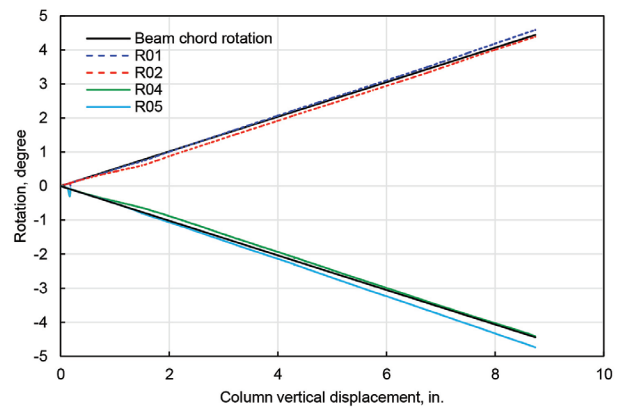


Threaded rod connection assembly

**Figure 7.** Vertical displacement profiles. Note:  $\theta$  = beam chord rotation. 1 in. = 25.4 mm.



Bolted connection assembly



Threaded rod connection assembly

**Figure 8.** Beam rotations. Note: R01 to R05 = inclinometers. 1 in. = 25.4 mm.

and that deformations were localized at the beam-to-column connections. The left part of Fig. 8 also shows the rotation of the column (R03), which began to rotate counterclockwise at approximately 3.00 in. (76 mm) of column vertical displacement. This counterclockwise rotation led to a concentration of axial deformation at the bottom-left anchor bolt, which eventually led to its rupture.

The right part of Fig. 8 shows inclinometer measurements from the threaded rod connection assembly, excluding R03, which malfunctioned during the test and did not produce meaningful data. In a manner similar to the beams in the bolted connection assembly test, the beams in the threaded rod connection assem-

bly rotated as rigid bodies, as indicated by the close agreement between the inclinometer measurements and beam chord rotation curves. The measured rotation near midspan of the right beam (R05) deviated the most from the beam chord rotation because it exceeded the beam chord rotation by 0.30 degrees, which is indicative of close agreement.

### Measured strains

Strain gauges on the stirrups of the bolted connection and threaded connection assembly beams (Fig. 2) recorded small strains, well below measurements that would indicate yield. Strain gauges in the bolted connection assembly beams indicat-

ed that flexural yielding of the beams did not occur. In contrast, flexural reinforcing steel at the bottom of the right beam in the threaded rod connection assembly yielded at a column vertical displacement of 2.30 in. (58 mm) and a beam chord rotation of 1.17 degrees. This initiation of yielding occurred near where the moment-rotation response transitioned from linear to non-linear (Fig. 5). A strain of 0.0026 was considered as indicative of yield in any reinforcing bar, assuming that the ASTM A706 Grade 60<sup>15</sup> (414 MPa) steel had a yield strength of 74 ksi (510 MPa) and an elastic modulus of 29,000 ksi (200 GPa).

Strain measurements at a cross section of the top thread bar in the right beam of the threaded rod connection assembly indicated that the thread bar was subjected to flexure. The magnitude of the tensile strain at the bottom side of the bar was nearly equal to the magnitude of the compressive strain at the top side of the bar. The top strain gauge on the top thread bar in the left beam malfunctioned, but it is inferred that this thread bar also underwent flexure because of symmetry in the assembly displacement profile. According to strain gauge measurements and force data from the through-hole compression load cells at the ends of the bars, the top thread bars remained elastic. The investigators considered a thread bar to have yielded at a strain of 0.0048, which was calculated by dividing the average yield strength by the average elastic modulus obtained from the previously described monotonic tension tests. The bottom thread bar in the left beam had tensile strains at the top and bottom of the bar. The top strain gauge had strain readings similar to those from the bottom strain gauge until it malfunctioned at approximately 2.00 in. (51 mm) of vertical column displacement. The bottom strain gauge functioned for the duration of the test and peaked at a strain of 0.07. The equal tensile strains at the top and bottom of the thread bar indicate that the bar was initially subjected to pure axial loading. Because the top strain gauge malfunctioned, it is unknown whether the bar stayed under a pure state of axial force for the remainder of the test.

## Robustness index

As defined in Eurocode 1, a structural system can be considered robust if it can “withstand events like fires, explosions, impact, or the consequences of human error, without being damaged to an extent disproportionate to the original cause.”<sup>24</sup> Many researchers have proposed frameworks or methodologies to quantify structural robustness, and a succinct review and discussion of many of these approaches can be found in Bao et al.<sup>25</sup> An energy-based framework that has been largely accepted in the research community was developed by Izzuddin et al.<sup>26</sup> In that framework, estimates of the capacity of a structural system under a dynamic loading scenario, such as sudden column loss, can be ascertained from a static pushdown test. The framework operates under the premise that at the instant when the maximum vertical displacement above the removed column is reached, the kinetic energy of the system is zero and the external work done by the gravity loading is equivalent to the internal energy (that is, the energy absorbed by the structure). Bao et al.<sup>25</sup> used this framework

in conjunction with aspects of other research to develop a robustness index  $R$ . They also presented a case study in which robustness indexes were calculated for two 10-story reinforced concrete buildings: one using intermediate moment frames and one using special moment frames. The robustness index of the special moment frame building was greater than that of the intermediate moment frame building, indicating that the stringent seismic design and detailing of the special moment frame building resulted in superior robustness against column loss.

The robustness index quantifies the ability of a structure to withstand gravity loading under sudden column loss, with values above unity indicating that the collapse will be arrested. The robustness index  $R$  for the bolted or threaded rod connection assembly can be calculated using the following equation:

$$R = \frac{1}{P_G \Delta_u} \int_0^{\Delta_u} P(\Delta) d\Delta$$

where

- $P_G$  = factored service-level gravity load acting on the unsupported column according to the extraordinary events load case ( $1.2D + 0.5L + A_k$ ) specified in ASCE 7-16<sup>13</sup>
- $\Delta_u$  = vertical displacement of the unsupported column corresponding to ultimate static load
- $\Delta$  = vertical displacement of the unsupported column
- $P(\Delta)$  = force-displacement relationship obtained from the static pushdown tests discussed in this paper

When calculating the robustness index  $R$ , the load or load effect resulting from the extraordinary event  $A_k$  equals 0 and plays no role in the determination of the factored service-level gravity load acting on the unsupported column according to the extraordinary events load case  $P_G$  because the load effect resulting from the extraordinary event (column loss) was physically considered in the testing by pushing down the unsupported column.

**Figure 9** shows the force-displacement curves up to connection failure of the bolted and threaded rod connection assemblies for both static loading and sudden column loss. The sudden column loss curves were derived by numerically integrating the static loading curves over the interval from zero to maximum column vertical displacement, normalizing by the column vertical displacement at each subinterval to obtain units of force and then plotting the normalized values as a function of the static column vertical displacement. The resistances of the bolted and threaded rod connection assemblies to sudden column loss are less than their resistances to static column loss because the resistances to sudden column loss account for the detrimental dynamic effects induced by sudden column loss. The ultimate capacities under sudden column loss were 68.8 and 64.5 kip (306 and 287 kN) for the bolted and threaded rod connec-

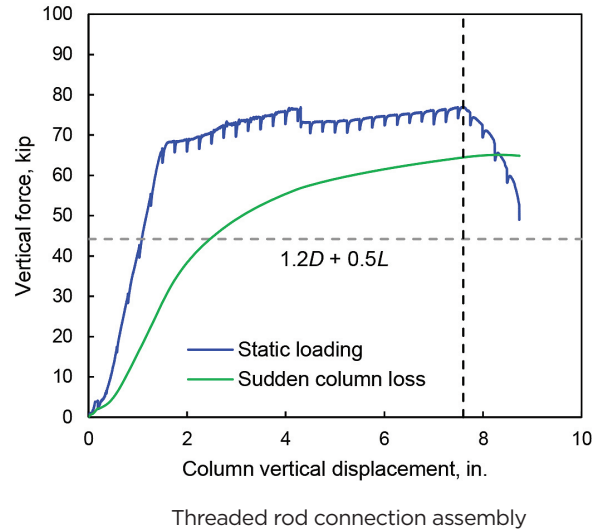
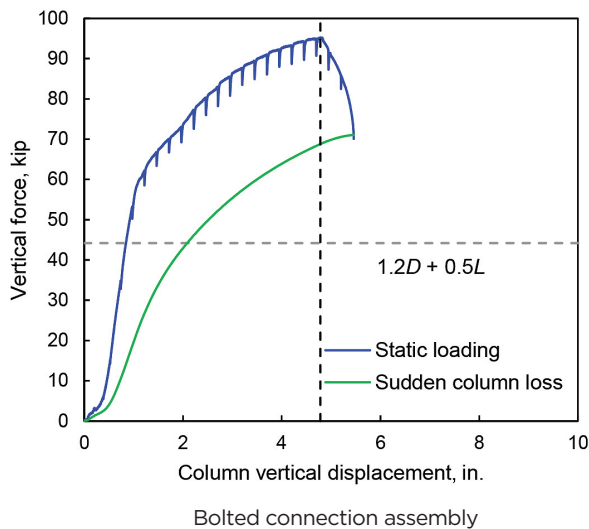


**Figure 9.** Force-displacement responses considering static loading and sudden column loss. Note:  $D$  = dead load;  $L$  = live load. 1 in. = 25.4 mm; 1 kip = 4.448 kN.

tion assemblies, respectively, as indicated by the point where the vertical dashed line intersects the sudden column-loss curves. The vertical dashed lines intersect the static loading curves at the points at which the ultimate capacity is achieved. Robustness indices of 1.6 and 1.5 were obtained for the bolted and threaded rod connection assemblies, respectively, by normalizing the sudden column loss capacities by the factored service-level gravity loading of 44.2 kip (197 kN), which is indicated by the horizontal dashed line. The robustness indexes for both assemblies indicate significant reserve capacity against collapse during sudden column loss under service-level gravity loads. The bolted and threaded rod connection assemblies could sustain loads 60% and 50% greater, respectively, than the 44.2 kip that they would need to sustain under sudden column loss to prevent collapse. These results are a vast improvement over the steel link plate connection performance reported by NIST,<sup>6</sup> where robustness indices of 1.02 and 1.11 were obtained from testing ordinary precast concrete moment frame and special precast concrete moment frame specimens, respectively.

## Conclusion

This paper presented results from static pushdown testing that simulated a column-removal scenario for disproportionate collapse applications for two precast concrete assemblies with novel moment connections that did not require the use of field welding. These connections were similar in concept in that they used anchor bolts or high-strength rods with pairs of threaded couplers embedded near the tops and bottoms of the respective columns. Based on the test results, the following main conclusions were reached:

- Both beam-to-column moment connection assemblies achieved the target design rotational capacity of 2.30 degrees

before reaching their ultimate moment strengths. The bolted connection assembly achieved an ultimate moment strength of 419 kip-ft (568 kN-m) at 2.43 degrees of beam chord rotation. The threaded rod connection assembly achieved an ultimate moment strength of 340 kip-ft (461 kN-m) at 3.87 degrees of beam chord rotation.

- The required moment strength stipulated by design was 234 kip-ft (317 kN-m). Both connection assemblies achieved this strength within their linear response region.
- For both connection assemblies, rotational deformations were localized at the beam-to-column connections as was intended by the design. The connection components (that is, anchor bolts and threaded rods) from both tests behaved as ductile fuses, and their rupture in tension was the mode of failure intended by the design.
- Robustness indices of 1.6 and 1.5 were obtained for the bolted and threaded rod connection assemblies, respectively, indicating that the assemblies could have sustained loads of 60% and 50% greater, respectively, than the 44.2 kip (197 kN) that they would need to sustain to prevent collapse under sudden column loss.
- In the laboratory, the threaded rod assembly's moment connections were easier to construct than those of the bolted connection assembly. The coarser threads and longer lengths of the thread bars provided the flexibility needed to establish the connections quickly and easily.

Care should be taken during the fabrication of these connections, with close attention paid to the steel couplers embedded in the column. The couplers should be level with no out-of-

plane skewness and should be secured before casting the concrete to ensure that they do not shift during casting. For the bolted connection, it is recommended that the anchor bolt threads be rolled instead of cut because rolled threads will likely be easier to mate with the coupling nuts embedded in the column. The process by which rolled threads are created results in threads that are typically free of surface imperfections and more resistant to damage, making them the preferred choice to ensure ease of construction in the field.

**Table 2** compares the performance metrics of both beam-to-column moment connection assemblies. The bolted connection had a larger ultimate moment strength and robustness index, whereas the threaded rod connection had a larger rotational capacity. Both connections exceeded their design moment strengths and target rotational capacities.

The test results suggested that both connection concepts are viable for use in precast concrete construction to achieve robust performance against disproportionate collapse. Both connection concepts eliminate costly field welding and the need for specialized labor. Because the connections can be made by hand, they are easier to make than typical welded precast concrete moment frame connections. Future research is needed to thoroughly quantify the potential cost savings that can be achieved when using these connections instead of welded ones. Further work is also required to quantify the long-term performance of both connection concepts and to gain an understanding of their behavior under loads induced by earthquakes and strong winds.

## Acknowledgments

The authors would like to thank PCI for its financial and technical support of this project. The authors also gratefully acknowledge Tindall Corp. for fabricating the specimens. Valuable input on the connection details was given by an industry review committee consisting of the following precast concrete experts: Greg Force (Tindall Corp.), Jared Brewe (former vice president of technical services at PCI), Roger Becker (retired PCI), Romany Gergious (Tindall Corp.), Isaac Perkins (Tindall Corp.), Michael Willis (Tindall Corp.), Andrew Osborn (Wiss, Janey, Elstner Associates Inc.), Craig Barrett (LEAP Associates International Inc.), Ned Cleland (Blue Ridge Design Inc.), Harry Gleich (Metromont Corp.), S. K. Ghosh (S. K. Ghosh and Associates Inc.), Sam Kakish (Enterprise Properties Inc.),

Walter Korkosz (The Consulting Engineers Group Inc.), Alex Mihaylov (Vector Structures), Clay Naito (Lehigh University), Spencer Quiel (Lehigh University), Perry Schram (Pennoni Associates Inc.), Kim Seeber (Seaboard Services of Virginia Inc.), and Aaron Vnuk (Precast Services Inc.).

## Disclaimer

Certain commercial entities, equipment, products, or materials are identified in this paper to describe a procedure or concept adequately. Such identification is not intended to imply recommendation or endorsement by the National Institute of Standards and Technology (NIST), nor is it intended to imply that the entities, equipment, products, or materials are necessarily the best available for the purpose. The findings and conclusions contained herein are those of the authors alone and do not reflect an official position of NIST or PCI.

## References

- Nair, R. S. 2004. "Progressive Collapse Basics." *Modern Steel Construction* 44 (3): 37–44.
- Popoff, A. 1975. "Design Against Progressive Collapse." *PCI Journal* 20 (2): 44–57. <https://doi.org/10.15554/pci.j.03011975.44.57>.
- Stevens, D., B. Crowder, D. Sunshine, K. Marchand, R. Smilowitz, E. Williamson, M. Waggoner. 2011. "DoD Research and Criteria for the Design of Buildings to Resist Progressive Collapse." *Journal of Structural Engineering* 137 (9): 870–880. [https://doi.org/10.1061/\(ASCE\)ST.1943-541X.0000432](https://doi.org/10.1061/(ASCE)ST.1943-541X.0000432).
- Lew, H. S., Y. Bao, F. Sadek, J. A. Main, S. Pujol, and M. A. Sozen. 2011. *An Experimental and Computational Study of Reinforced Concrete Assemblies under a Column Removal Scenario*. NIST (National Institute of Standards and Technology) Technical Note 1720. Gaithersburg, MD: NIST. <https://doi.org/10.6028/NIST.TN.1720>.
- Sadek, F., J. A. Main, H. S. Lew, S. D. Robert, V. P. Chiarito, and S. El-Tawil. 2010. *An Experimental and Computational Study of Steel Moment Connections Under a Column Removal Scenario*. NIST Technical Note 1669. Gaithersburg, MD: NIST. <https://doi.org/10.6028/nist.tn.1669>.
- Main, J. A., Y. Bao, H. S. Lew, F. Sadek, V. Chiarito, S. D. Robert, and J. Torres. 2015. *An Experimental and Computational Study of Precast Concrete Moment Frames under a Column Removal Scenario*. NIST Technical Note 1886. Gaithersburg, MD: NIST. <https://doi.org/10.6028/NIST.TN.1886>.
- PCI. 2010. *PCI Design Handbook: Precast and Prestressed Concrete*. 7th ed. MNL 120-10, Chicago, IL: <https://doi.org/10.15554/MNL-120-10>.

**Table 2.** Summary of important performance metrics

Performance metric	Bolted connection	Threaded rod connection
Ultimate moment strength, kip-ft	419	340
Rotational capacity, degrees	2.43	3.87
Robustness index	1.6	1.5

Note: 1 kip-ft = 1.356 kN-m.

8. French, C. W., M. Hafner, V. Jayashankar. 1989. "Connection between Precast Elements—Failure within Connection Region." *Journal of Structural Engineering* 115 (12): 3171–3192. [https://doi.org/10.1061/\(ASCE\)0733-9445\(1989\)115:12\(3171\)](https://doi.org/10.1061/(ASCE)0733-9445(1989)115:12(3171)).
9. French, C. W., M. Hafner, V. Jayashankar. 1989. "Connection Between Precast Elements—Failure outside Connection Region." *Journal of Structural Engineering* 115 (2): 316–340. [https://doi.org/10.1061/\(ASCE\)0733-9445\(1989\)115:2\(316\)](https://doi.org/10.1061/(ASCE)0733-9445(1989)115:2(316)).
10. Quiel, S. E., C. J. Naito, and C. T. Fallon. 2019. "A Non-emulative Moment Connection for Progressive Collapse Resistance in Precast Concrete Building Frames." *Engineering Structures*, no. 179, 174–188. <https://doi.org/10.1016/j.engstruct.2018.10.027>.
11. Kim, J., P. Dasgupta, S. K. Ghosh. 2009. *Assessment of the Ability of Seismic Structural Systems to Withstand Progressive Collapse: Design of Precast Concrete Frame Building (Seismic Design Category D)*. Report submitted to the National Institute of Standards and Technology. Gaithersburg, MD: NIST.
12. ASCE (American Society of Civil Engineers). 2005. *Minimum Design Loads for Buildings and Other Structures*. SEI/ASCE 7-05. Reston, VA: ASCE.
13. ASCE. 2016. *Minimum Design Loads for Buildings and Other Structures*. SEI/ASCE 7-16. Reston, VA: ASCE.
14. U.S. Department of Defense. 2016. *Design of Buildings to Resist Progressive Collapse*. UFC 4-023-03. Washington, DC: U.S. Department of Defense.
15. ASTM International. 2022. *Standard Specification for Deformed and Plain Low-Alloy Steel Bars for Concrete Reinforcement*. ASTM A706/A706M-22. West Conshohocken, PA: ASTM International.
16. PCI. 2017. *PCI Design Handbook: Precast and Prestressed Concrete*. 8th ed. MNL 120-17. Chicago, IL: <https://doi.org/10.15554/MNL-120-17>.
17. ASTM International. 2020. *Standard Specification for Anchor Bolts, Steel, 36, 55, and 105-ksi Yield Strength*. ASTM F1554-20. West Conshohocken, PA: ASTM International.
18. ACI (American Concrete Institute). 2005 (reapproved 2019). *Acceptance Criteria for Moment Frames Based on Structural Testing and Commentary*. ACI 374.1-05(19). Farmington Hills, MI: ACI.
19. ASTM International. 2019. *Standard Specification for Carbon Structural Steel*. ASTM A36/A36M-19. West Conshohocken, PA: ASTM International.
20. ASTM International. 2018. *Standard Specification for High-Strength Steel Bars for Prestressed Concrete*. ASTM A722/A722M-18. West Conshohocken, PA: ASTM International.
21. ASTM International. 2021. *Standard Test Method for Compressive Strength of Cylindrical Concrete Specimens*. ASTM C39/C39M-21. West Conshohocken, PA: ASTM International.
22. ASTM International. 2021. *Standard Test Method for Compressive Strength of Hydraulic Cement Mortars (Using 2-in. or [50 mm] Cube Specimens)*. ASTM C109/C109M-21. West Conshohocken, PA: ASTM International.
23. ASTM International. 2020. *Standard Specification for Packaged Dry, Hydraulic-Cement Grout (Nonshrink)*. ASTM C1107/C1107M-20. West Conshohocken, PA: ASTM International.
24. CEN (European Committee for Standardization). 2006. *Eurocode 1: Actions on Structures—Part 1–7: General Actions—Accidental Actions*. Brussels, Belgium: CEN.
25. Bao, Y., J. A. Main, S. Y. Noh. 2017. "Evaluation of Structural Robustness against Column Loss: Methodology and Application to RC Frame Buildings." *Journal of Structural Engineering* 143 (8): 04017066. [https://doi.org/10.1061/\(ASCE\)ST.1943-541X.0001795](https://doi.org/10.1061/(ASCE)ST.1943-541X.0001795).
26. Izzuddin, B. A., A. G. Vlassis, A. Y. Elghazouli, and D. A. Nethercot. 2008. "Progressive Collapse of Multi-Storey Buildings Due to Sudden Column Loss—Part I: Simplified Assessment Framework." *Engineering Structures* 30 (5): 1308–1318. <https://doi.org/10.1016/j.engstruct.2007.07.011>.

## Notation

$A_k$	= load or load effect arising from extraordinary event A
$D$	= dead load
$k$	= coverage factor
$L$	= live load
$L_1$	= horizontal distance from centerline of column to centerline of pin
$n$	= number of independent measurements
$P_G$	= factored service-level gravity load
$P(\Delta)$	= force-displacement relationship obtained from the static pushdown tests

$R$	= robustness index
$S_L$	= length scale
$S_M$	= moment demand scale
$S_\sigma$	= stress scale
$u_c$	= sample standard deviation
$U$	= expanded uncertainty
$\delta$	= average of vertical displacement measurements D05 and D06
$\Delta$	= vertical displacement of the unsupported column
$\Delta_u$	= vertical displacement of the unsupported column corresponding to ultimate static load
$\theta$	= beam chord rotation
$\mu$	= mean value

## About the authors



Malcolm Ammons, PhD, is a research structural engineer at the National Institute of Standards and Technology in Gaithersburg, Md.



Jonathan Weigand, PhD, is a research structural engineer at the National Institute of Standards and Technology.



Majd Hijazi is a PhD candidate in the Department of Civil and Environmental Engineering at The Catholic University of America in Washington, D.C.



Travis Thonstad, PhD, is an assistant professor in the Department of Civil and Environmental Engineering at the University of Washington in Seattle, Wash.

## Abstract

This paper presents an experimental study of two precast concrete moment frame assemblies tested under a notional column-removal scenario. The assemblies were derived at a five-eighth scale from a 10-story prototype building and consisted of two spandrel beams connected to a central column. The unsupported column was subjected to monotonically increasing vertical displacement until connection failure. Moment connections in both assemblies were made using either anchor bolts or high-strength threaded rods, which were threaded into couplers embedded near the tops and bottoms of the respective columns to complete the connections. The connection components were centered on the thickness of the beams to limit the eccentricity of the tensile force transfer path. Both connection assemblies failed from the rupture of one of the anchor bolts or threaded rods at the bottom connection. An energy-based analysis of the test results revealed that both connections had a similar reserve capacity against collapse under sudden column loss.

The connections did not require field welding and were easily constructed in the laboratory. They also demonstrated improved reserve capacity against collapse under sudden column loss compared with conventional steel link plate moment connections. These advantages suggest the viability of these connections for use in precast concrete construction.

## Keywords

Column removal, disproportionate collapse, moment connections, robustness.

## Review policy

This paper was reviewed in accordance with the Precast/Prestressed Concrete Institute's peer-review process. The Precast/Prestressed Concrete Institute is not responsible for statements made by authors of papers in *PCI Journal*. No payment is offered.

## Publishing details

This paper appears in *PCI Journal* (ISSN 0887-9672) V. 70, No. 4, July–August 2025, and can be found at <https://doi.org/10.15554/pcij70.4-01>. *PCI Journal* is published bimonthly by the Precast/Prestressed Concrete Institute, 8770 W. Bryn Mawr Ave., Suite 1150, Chicago, IL 60631. Copyright © 2025, Precast/Prestressed Concrete Institute.

## Reader comments

Please address any reader comments to *PCI Journal* editor-in-chief Tom Klemens at [tklemens@pci.org](mailto:tklemens@pci.org) or Precast/Prestressed Concrete Institute, c/o *PCI Journal*, 8770 W. Bryn Mawr Ave., Suite 1150, Chicago, IL 60631.